The Gene *sml0013* of *Synechocystis* Species Strain PCC 6803 Encodes for a Novel Subunit of the NAD(P)H Oxidoreductase or Complex I That Is Ubiquitously Distributed among Cyanobacteria[1][W]

Doreen Schwarz, Hendrik Schubert, Jens Georg, Wolfgang R. Hess, and Martin Hagemann*

University of Rostock, Institute of Biosciences, Department of Plant Physiology (D.S., M.H.) and Department of Ecology (H.S.), D–18059 Rostock, Germany; and University of Freiburg, Faculty of Biology, Genetics, and Experimental Bioinformatics, D–79104 Freiburg, Germany (J.G., W.R.H.)

The NAD(P)H oxidoreductase or complex I (NDH1) complex participates in many processes such as respiration, cyclic electron flow, and inorganic carbon concentration in the cyanobacterial cell. Despite immense progress in our understanding of the structure-function relation of the cyanobacterial NDH1 complex, the subunits catalyzing NAD(P)H docking and oxidation are still missing. The gene *sml0013* of *Synechocystis* 6803 encodes for a small protein of unknown function for which homologs exist in all completely known cyanobacterial genomes. The protein exhibits weak similarities to the NDH-dependent flow6 (NDF6) protein, which was reported from Arabidopsis (*Arabidopsis thaliana*) chloroplasts as a NDH subunit. An *sml0013* inactivation mutant of *Synechocystis* 6803 was generated and characterized. It showed only weak differences regarding growth and pigmentation in various culture conditions; most remarkably, it exhibited a glucose-sensitive phenotype in the light. The genome-wide expression pattern of the Δ*sml0013*::Km mutant was almost identical to the wild type when grown under high CO_2 conditions as well as after shifts to low CO_2 conditions. However, measurements of the photosystem I redox kinetic in cells of the Δ*sml0013*::Km mutant revealed differences, such as a decreased capability of cyclic electron flow as well as electron flow into respiration in comparison with the wild type. These results suggest that the Sml0013 protein (named NdhP) represents a novel subunit of the cyanobacterial NDH1 complex, mediating its coupling either to the respiratory or the photosynthetic electron flow.

Cyanobacteria are the only photolithoautotrophic prokaryotes performing oxygenic photosynthesis. As in plant chloroplasts, the light reactions are situated on an internal membrane system, the thylakoids. Linear electron flow starts at PSII connected to the water-splitting center and transfers electrons via the cytochrome b_6f ($Cytb_6f$) complex and PSI to $NADP^+$. Additionally, cyanobacteria are able to perform cyclic electron flow around PSI, producing only ATP. These light reactions allow cyanobacteria to obtain the necessary energy and reductants at varying levels in the light. In the dark, cyanobacteria also perform a respiratory electron transport to fulfill energy demands at the expense of stored carbohydrates, usually glycogen. As in heterotrophic bacteria, electrons from $NAD(P)H+H^+$ are fed into the respiratory chain via the NAD(P)H oxidoreductase or complex I (NDH1). However, the cyanobacterial respiratory and photosynthetic electron transport chains are linked (i.e. both use several electron carriers together, such as the $Cytb_6f$ complex and mobile electron carriers). The lumenal electron carriers cytochrome *c* (Cytc) and plastocyanin donate electrons not only to PSI but also to the respiratory terminal cytochrome oxidase (Cytox), usually of the aa3 type, where oxygen is reduced back to water. The proton gradient generated via respiratory or photosynthetic electron transport is used by the ATPase to generate ATP (Bryant, 1994).

It has been shown that distinct, strain-dependent differences exist depending on which respiratory and photosynthetic electron flow routes are interconnected or more separated. In strains such as our model, *Synechocystis* sp. PCC 6803 (hereafter *Synechocystis* 6803), the complete respiratory chain is localized on thylakoids, whereas in cyanobacteria such as *Synechococcus elongatus* PCC 7942, the respiratory chain is more separated on the cytoplasmic membrane from the thylakoid-localized photosynthetic chain (Peschek et al., 1994). To acclimate toward different environmental conditions, the cyanobacterial electron transfer network shows a relatively high degree of flexibility not only in its activity but also in its composition. For example, the preference for plastocyanin under copper-replete conditions switches to Cytc under copper-deplete conditions, while iron limitation results in a switch from the iron-containing ferredoxin to flavodoxin (Hagemann et al., 1999). The

[1] This work was supported by the Deutsche Forschungsgemeinschaft (grant to M.H.).

* Address correspondence to martin.hagemann@uni-rostock.de.

The author responsible for distribution of materials integral to the findings presented in this article in accordance with the policy described in the Instructions for Authors (www.plantphysiol.org) is: Martin Hagemann (martin.hagemann@uni-rostock.de).

[W] The online version of this article contains Web-only data.

www.plantphysiol.org/cgi/doi/10.1104/pp.113.224287

cyclic electron flow around PSI can use different routes, mainly via NDH1 but also directly to $Cytb_6f$ (Yeremenko et al., 2005). Finally, respiratory electron transport also can be connected to three different terminal oxidases depending on strain or growth conditions (Pils and Schmetterer, 2001).

Particularly high functional as well as structural diversity was shown for the cyanobacterial NDH1 complex (Zhang et al., 2004). As in other bacteria, it is involved in respiration, transferring electrons from carbohydrate catabolism into the plastoquinone (PQ) pool (Haimovich-Dayan et al., 2011). However, NDH1 also is involved in the cyclic electron flow around PSI (Yeremenko et al., 2005; Bernát et al., 2011). These two NDH1 functions are conserved in the chloroplastidial NDH complex that is phylogenetically derived from the cyanobacterial one (Ifuku et al., 2011). Moreover, it also has been established that NDH1 is essential for the CO_2 conversion into HCO_3^- as part of the cyanobacterial inorganic carbon-concentrating mechanism (Ogawa, 1991; Shibata et al., 2001). This functional diversity is reflected in a structural diversity thought to serve these different purposes. For example, many of the smaller NDH1 subunits are encoded by multigene families (e.g. *ndhF* or *ndhD*), which are differentially expressed under changing conditions such as high or low CO_2. The expression changes result in the generation of differently sized NDH1 complexes with different subunit composition, which can preferentially function in respiratory electron transport and cyclic electron transfer around PSI (called NDH1L) or in the conversion of CO_2 into HCO_3^- (called NDH1MS; Zhang et al., 2004). Despite intensive investigations on the cyanobacterial as well as the chloroplastidial NDH1 complexes, the subunits for NAD(P)H oxidation are still unknown, making the functioning of these complexes enigmatic (for review, see Battchikova et al., 2011a). Recent isolations of functional NDH complexes from *Thermosynechococcus elongatus* indicated that reduced ferredoxin could possibly directly transfer electrons via ferredoxin-$NADP^+$ oxidoreductase to NDH1 (Hu et al., 2013).

Accordingly, genome searches or proteomic analyses of isolated NDH1 complexes have often been used to gain more insights into the function of the NDH1 complex. A new NDH subunit was found in chloroplasts, named NDH-dependent flow6 (NDF6; Ishikawa et al., 2008). A protein called NdhP displaying weak similarities to NDF6 was recently copurified with active NDH1 complexes from the cyanobacterium *T. elongatus* (Nowaczyk et al., 2011). Here, we report on the generation and characterization of the mutant Δ*sml0013*::Km, in which the NDF6 homolog Sml0013 of *Synechocystis* 6803 was inactivated.

RESULTS AND DISCUSSION

Sequence Analysis

The gene *sml0013* encodes for a small protein of only 40 amino acid residues. Initial BLAST-P analysis disclosed the presence of Sml0013-like proteins in the genomes of all cyanobacteria sequenced to date, including the marine picoplanktonic cyanobacteria of the genera *Prochlorococcus* and *Synechococcus*, which are characterized by a strongly reduced genome size (Scanlan et al., 2009; Larsson et al., 2011). In all genomes, these proteins are annotated as hypothetical proteins of unknown function. Moreover, proteins with similarities to Sml0013 are also encoded in the genomes of some cyanophages, for example, the *Prochlorococcus* phage P-SSM2 (Supplemental Fig. S1), as was already reported by Cobley (2010). A closer look into the genome organization and sequences allowed distinguishing three groups of Sml0013-like proteins among cyanobacteria. Their distribution correlates with the three major cyanobacterial clades defined by Gupta and Mathews (2010). Among basal cyanobacteria of clade A, such as *Gloeobacter violaceus* PCC 7421, these proteins are found as single genes. In all genomes of clade B cyanobacteria, such as *Synechocystis* 6803, they are linked to a gene encoding a protein belonging to the COG1236 class with a β-lactamase fold, predicted as exonuclease involved in RNA processing. There exists a GenBank accession reporting that the mutation of this gene resulted in a changed phycobilisome content in the cyanobacterium *Microchaeta diplosiphon* (ABB88926.1). Finally, among the clade C cyanobacteria comprising mostly marine picoplanktonic strains, the Sml0013 homolog is encoded upstream of a gene for putative amidases/creatinases (Supplemental Fig. S1). The ubiquitous distribution and the highly conserved sequence and genome organization suggest a meaningful role of Sml0013-like proteins among cyanobacteria.

Extended similarity searches with entries of the entire National Center for Biotechnology Information database identified further proteins (NDF6-like) among plants displaying low degrees of similarity toward the cyanobacterial Sml0013-like proteins. The nucleus-encoded protein NDF6 was first identified in chloroplasts of Arabidopsis (*Arabidopsis thaliana*) and shown to be functionally associated with the chloroplastidial NDH complex (Ishikawa et al., 2008). Accordingly, the protein was named NDF6 for the NAD(P)H dehydrogenase (NDH)-dependent flow6 superfamily (PLN00180 in the Conserved Domain Database) of land plants such as Arabidopsis, rice (*Oryza sativa*), grape (*Vitis vinifera*), and *Populus trichocarpa* (Ishikawa et al., 2008). However, the plant NDF6-like proteins are much larger than the similar proteins from cyanobacteria (Supplemental Fig. S2). Even after removing the N-terminal transit peptide for chloroplast import, the mature proteins in chloroplasts show an approximately 60-amino acid extension at the N terminus and a 40-amino acid extension at the C terminus. Thus, only the highly conserved central part of the plant NDF6-like proteins displays the similarities to the cyanobacterial Sml0013-like proteins. This part of the proteins contains a hydrophobic stretch, which possibly forms a membrane-spanning helix (Ishikawa et al., 2008). Interestingly, the similarity

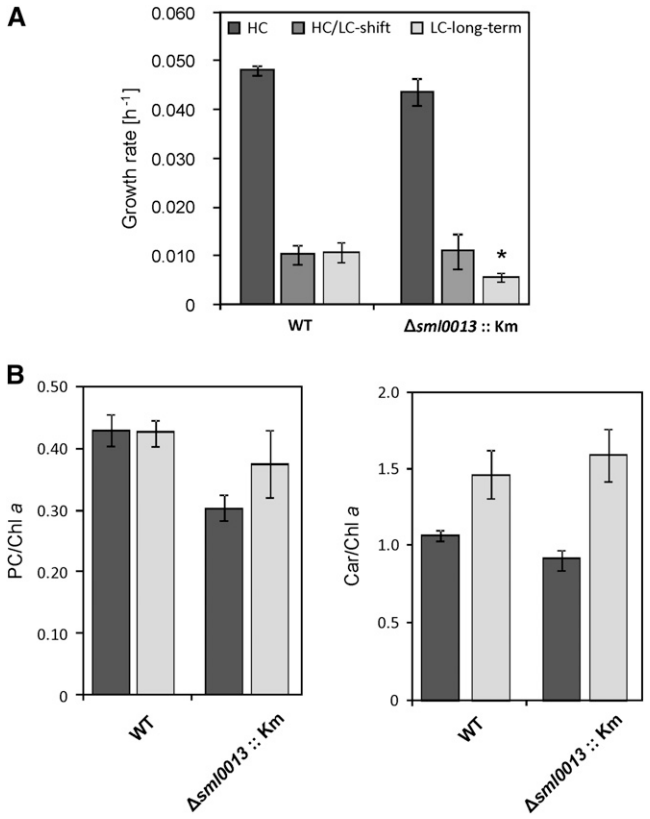

Figure 1. Growth and pigmentation of cells cultivated under HC (5% CO_2) or LC (0.035% CO_2) conditions. A, Growth rates after cultivation under HC conditions, 24 h after shifting HC precultivated cells to LC, or after long-term LC acclimation. B, Pigmentation ratios of phycocyanin (PC) and carotenoids (Car) relative to chlorophyll *a* (Chl *a*) in HC-grown (dark gray columns) and long-term LC-acclimated (light gray columns) cells. Mean values and SD are shown. A statistically significant difference of mutant data in comparison with wild-type data (WT) is indicated by the asterisk ($P \leq 0.05$).

of another small subunit of the NDH1 in cyanobacteria (NdhS) and chloroplasts (CRR31) also was restricted to the central part of the much larger chloroplastidial protein (Battchikova et al., 2011b), which forms in CRR31 a domain displaying some similarities to PsaE involved in ferredoxin binding at PSI (Yamamoto et al., 2011). The first evidence that the NDF6-like proteins among cyanobacteria are really associated with NDH1 was provided by Nowaczyk et al. (2011), who identified an Sml0013 homolog in purified NDH1 complexes from *T. elongatus*. These findings suggest that the Sml0013 protein also might be associated with the NDH1 complex. To investigate the function of this small protein, we generated the Δ*sml0013*::Km mutant of *Synechocystis* 6803 (Supplemental Fig. S3).

Characterization of Growth

Insertion mutagenesis of *sml0013* allowed the generation of many independent kanamycin (Km)-resistant clones, which showed the complete absence of the wild-type gene (Supplemental Fig. S3; Supplemental Table S1). This finding indicates that the Sml0013 protein is not essential under our standard growth conditions. To rule out polar effects, we generated an insertion mutant, Δ*sll0514*::SmI, and a deletion mutant, Δ*sll0514*::SmD, which were solely affected in the downstream open reading frame (ORF) *sll0514* (Supplemental Fig. S4). Subsequently, the growth of the mutant clones and the wild type was compared under different conditions, including varying inorganic carbon amounts, inorganic nitrogen sources and amounts, light regimes, or temperatures. In most of the cases, wild-type and mutant cells behaved similarly (data not shown). Since it is known that the NDH1 is important for inorganic carbon uptake, we analyzed the behavior of these strains toward varying CO_2 concentrations in more detail. Similar growth rates were found for the *Synechocystis* 6803 mutant Δ*sml0013*::Km compared with the wild type at high CO_2 (5%; HC) or 24 h after the shift to low CO_2 (0.038%; LC), whereas long-term cultivation at LC decreased the growth of Δ*sml0013*::Km cells (Fig. 1). Despite the similar growth, mutant cells were characterized by a lowered content of phycocyanin and carotenoids at HC, whereas pigmentation was not significantly different under LC conditions.

The exposure to different light regimes, continuous light, light/dark changes, or light-activated heterotrophic growth (LAHG), also did not result in any significant differences between mutant and wild-type cells (Fig. 2). In contrast, the addition of Glc to the

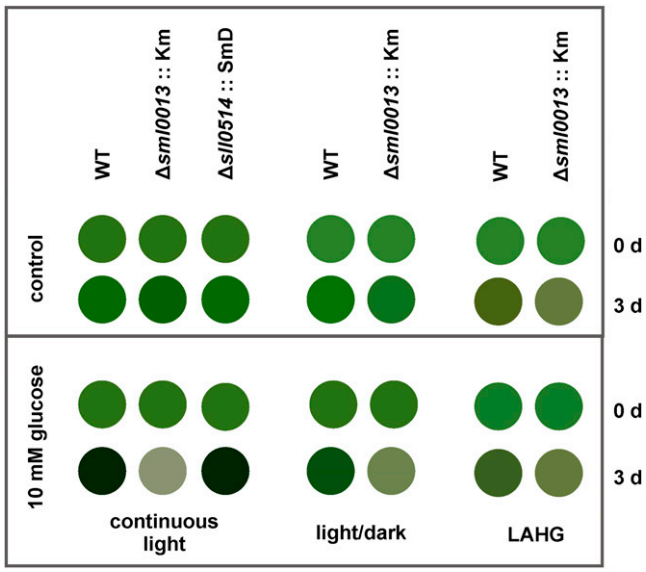

Figure 2. Appearance of the *Synechocystis* 6803 wild type (WT) or mutant Δ*sml0013*::Km as well as mutant Δ*sll0514*::SmD after growth under different light regimes in the absence (control) or presence of 10 mM Glc. Axenic cultures of the wild type or mutants were cultivated in continuous light, light/dark changes, or LAHG under LC conditions for 3 d.

medium revealed a Glc-sensitive phenotype of the *Synechocystis* 6803 mutant Δ*sml0013*::Km when cultivated in flasks without CO_2 supplementation. The strength of the phenotype became enhanced by the presence of light. Under continuous illumination, cells of the mutant Δ*sml0013*::Km lysed 3 d after the addition of 10 mM Glc. If the Δ*sml0013*::Km cells were cultivated with Glc under light/dark conditions, the growth became clearly diminished but Glc was not toxic, whereas no Glc effect was detected when cells were incubated under LAHG conditions. The mutants with defects in the downstream ORF *sll0514* did not show the Glc-sensitive phenotype of the mutant Δ*sml0013*::Km (Fig. 2). Moreover, precultivation at HC in the presence of Glc resulted in the release of a brownish compound into the medium by Δ*sml0013*::Km cells, indicating stress. However, the cells survived and grew at almost the same rate as the wild type (growth rates of $0.024 \pm 0.001\ h^{-1}$ and $0.019 \pm 0.003\ h^{-1}$ for the wild type and mutant Δ*sml0013*::Km, respectively). The *Synechocystis* 6803 wild-type strain used in this work is characterized by the ability to take up and utilize external Glc as a carbon resource. Accordingly, the growth of the wild type was stimulated by Glc at all light regimes (Fig. 2). Many different Glc-sensitive mutants of *Synechocystis* 6803 have been characterized in recent years (for review, see Haimovich-Dayan et al., 2011). Among them, mutants with defective NDH1 were found.

Gene Expression Changes

The genome-wide transcriptional changes in response to HC/LC shifts were compared between cells of the wild type and the mutant Δ*sml0013*::Km. As reported before by Wang et al. (2004) and Eisenhut et al. (2007), shifts from HC into LC increased the transcript level of many genes, including those for inorganic carbon transport systems like SbtA (*slr1512/slr1513* operon), BCT1 (*slr0040-0044* operon), and NDH1MS (*slr2006-2013* and *sll1732-1736* operon; Table I). Many other genes also were found to be LC induced, for example, the *flv* operon (*sll0217-sll0219*; a graphical representation of the fold change values for each probe is provided in Supplemental File S1; the complete microarray data set is accessible in the Gene Expression Omnibus [GEO] database under accession no. GSE48415). The genes for the constitutive BicA transporter as well as subunits of the NDH1 complex showed only minor changes in both strains (Table I). Other NDH subunits also did not show any signs of an up- or down-regulation in cells of the wild type and the mutant Δ*sml0013*::Km, which is supposed to be affected in an NDH1 subunit. Generally, the DNA microarray data set revealed that the removal of the gene *sml0013* had only minor impact on the overall gene expression pattern under HC or HC/LC shift conditions in comparison with the wild type.

Table I. *Selected LC-inducible genes in cells of the Synechocystis 6803 wild type or mutant Δsml0013::Km*

RNA was isolated from cells grown at HC conditions or after a shift from HC to LC for 24 h. The relative expression (fold change) of these genes is given for wild-type cells (wild-type LC/wild-type HC) and cells of the mutant (Δ*sml0013* LC/Δ*sml0013* HC). Changes of 1.87-fold or greater and 0.53-fold or less (boldface) indicate significantly increased or decreased transcript levels.

Function	ORF	Gene Name	Wild-Type LC/Wild-Type HC	Δ*sml0013* LC/Δ*sml0013* HC
			fold change	
Inorganic carbon transporter				
BCT1	*slr0040*	*cmpA*	**15.03**	**19.89**
	slr0041	*cmpB*	**14.81**	**18.21**
	slr0042	*porB*	**12.87**	**14.93**
	slr0043	*cmpC*	**8.13**	**10.26**
	slr0044	*cmpD*	**9.60**	**10.93**
	sll0030	*cmpR*	1.41	1.40
SbtA	*slr1512*	*sbtA*	**17.33**	**24.06**
	slr1513	*sbtB*	**9.56**	**11.13**
$NDH1_3$	*sll1732*	*ndhF3*	**23.02**	**25.71**
	sll1733	*ndhD3*	**18.02**	**20.55**
	sll1734	*cupA*	**11.65**	**13.25**
	sll1735		**7.62**	**7.71**
	sll1736		**2.55**	**3.81**
	sll1594	*ndhR*	**4.24**	**2.80**
$NDH1_4$	*sll0026*	*ndhF4*	0.68	0.68
	sll0027	*ndhD4*	1.17	**2.09**
	slr1302	*cupB*	**0.42**	**0.33**
BicA	*sll0834*	*bicA*	0.76	0.86
Flavoprotein				
flv operon	*sll0217*	*dfa2*	**41.85**	**47.32**
	sll0218		**43.72**	**42.40**
	sll0219	*dfa4*	**38.32**	**35.48**

However, a few significant gene expression changes were observed between wild-type and mutant cells. Increased mRNA levels were detected for 11 genes and decreased levels were detected for 14 genes under HC or HC/LC shift conditions (Table II). In addition, increased levels were detected for 18 noncoding and antisense RNAs and decreased levels were detected for four antisense RNAs (Supplemental Table S2). Among the latter are the antisense RNAs to *flv4* (*sll0217*), consistent with the relatively decreased mRNA level of *flv4* (Table II), supporting the control function of this antisense RNA (Eisenhut et al., 2012). Interestingly, *ssr2016* was found among the genes with increased transcript levels. This gene encodes for a protein with low similarity to Pgr5, a protein known from land plants to be involved in the cyclic electron flow around PSI (Munekage et al., 2002). It has been shown that the *ssr2016* mutant of *Synechocystis* 6803 also was affected in the antimycin A-sensitive route of cyclic electron transport, which acts independently from the NDH1 complex-mediated route (Yeremenko et al., 2005). Expression of the ATPase operon also was stimulated in mutant cells, which might indicate a decrease in the energy production of this strain. Potential imbalance in photosynthetic energy utilization in mutant cells also is mirrored by the increased expression level of *ssr2595*. This gene codes for HliB or ScpD, a small chlorophyll-binding protein that was found to be induced under high light, oxygen, and many other stresses affecting the growth of *Synechocystis* 6803 (Funk and Vermaas, 1999; Los et al., 2008; Engelken et al., 2012). In contrast to genes with elevated transcription, most of the genes characterized by a lowered expression level in mutant cells relative to the wild type code for proteins with unknown functions (Table II). The *sml0013* gene, which was inactivated in the mutant Δ*sml0013*::Km, showed the highest degree of diminished mRNA level, serving as a good control. Three of the repressed genes code for proteins that are known to be activated during nitrogen starvation (Aguirre von Wobeser et al., 2011). The NblA1 and NblA2 proteins are crucial for the degradation of phycobilisomes in the process of chlorosis after nitrogen starvation (Collier and Grossman, 1994; Baier et al., 2001), whereas the GifA protein together with GifB acts as a negative regulator for Gln synthetase, one of the main ammonia-assimilating

Table II. *Complete list of genes showing significant transcriptional changes in cells of the Synechocystis 6803 mutant Δsml0013::Km relative to the wild type*

The relative expression (fold change) of these genes is given for HC-grown cells (Δ*sml0013* HC/wild-type HC) and cells shifted from HC into LC (Δ*sml0013* LC/wild-type LC) for 24 h. Changes of 1.87-fold or greater and 0.53-fold or less indicate significantly increased or decreased transcript levels.

ORF	Gene	Annotation	Δ*sml0013* HC/Wild-Type HC	Δ*sml0013* LC/Wild-Type LC
			fold change	
Increased expression				
slr0798	*ziaA*	Zinc-transporting P-type ATPase (zinc efflux pump) involved in zinc tolerance	**3.95**	0.77
ssr2595	*hliB*	High light-inducible polypeptide HliB	**1.93**	0.81
ssr2016	*pgr5*	Hypothetical protein	**1.92**	0.82
sll1322	*atpB*	ATP synthase B chain	0.99	**1.90**
sll1323	*atpG*	ATP synthase G chain	1.03	**1.99**
sll1324	*atpF*	ATP synthase F chain	1.04	**1.89**
ssl2615	*atpH*	ATP synthase C chain	1.09	**2.28**
slr0447	*urtA*	ABC-type urea transport system substrate-binding protein	1.12	**2.01**
sll1325	*atpD*	ATP synthase δ-chain	1.06	**1.99**
slr1756	*glnA*	Gln synthetase	1.10	**1.88**
sll1688		Hypothetical protein	**1.92**	0.82
Decreased expression				
slr1957		Hypothetical protein	**0.47**	0.68
sll1898	*ctaA*	Hypothetical protein	**0.48**	0.70
sll0514		Hypothetical protein	**0.40**	**0.44**
ssr2062		Hypothetical protein	**0.39**	**0.46**
ssl1911	*gifA*	Gln synthetase-inactivating factor IF7	**0.38**	0.89
slr1634		Hypothetical protein	**0.31**	0.96
sll1862		Hypothetical protein	0.76	**0.45**
slr0442		Hypothetical protein	1.07	**0.41**
sll1695	*pilA2*	Pilin polypeptide PilA2	1.13	**0.33**
sll1696		Hypothetical protein	1.05	**0.42**
ssl0452	*nblA1*	Phycobilisome degradation protein NblA1	1.39	**0.35**
ssl0453	*nblA2*	Phycobilisome degradation protein NblA2	1.37	**0.50**
sll1689	*sigE*	Alternative σ-factor SigE	**0.48**	0.73
sml0013	*ndhP*	Hypothetical protein	**0.17**	**0.14**

enzymes (Garcia-Domínguez et al., 2000). Consistent with the decreased expression of *gifA*, an increased expression of *glnA* for Gln synthetase was detected (Table II). Together with the observed decreased phycocyanin/chlorophyll *a* ratio (Fig. 1B), the increased level of *glnA* mRNA and the decreased mRNA levels of *nblA1*, *nblA2*, and *gifA* can be taken as evidence that the nitrogen assimilation also is slightly affected in the mutant. However, as the general response to the shift from HC to LC was found to be intact, we interpret the gene expression changes between wild-type and mutant cells to be caused by the physiological response to lacking the Sml0013 protein.

NDH Activity Measurement via PSII Fluorescence

To get evidence that the Sml0013 protein is functionally associated with NDH1, we monitored the postillumination rise in chlorophyll *a* fluorescence. This parameter is often used as a measure for the rate of NDH1-based cyclic electron transport rates in cyanobacteria (Battchikova et al., 2011b) or in chloroplasts (Ishikawa et al., 2008). Our measurements revealed a small postillumination rise in cells of the wild type when grown under HC, which was almost absent in the mutant Δ*sml0013*::Km under the same conditions (Fig. 3). In contrast, LC-acclimated cells of the wild type and Δ*sml0013*::Km showed a much larger increase in PSII fluorescence after switching off the actinic light. It has been shown that acclimation to low CO_2 supply increases the amount and composition of NDH1 subunits as well as the rate of PSI cyclic electron transport (Wang et al., 2004; Zhang et al., 2004; Eisenhut et al., 2007). Accordingly, our data imply that the absence of Sml0013 is mostly affecting the NDH1L complex that dominates under HC, while the NDH1MS complexes for CO_2 uptake, especially under LC, are rather not affected by this mutation.

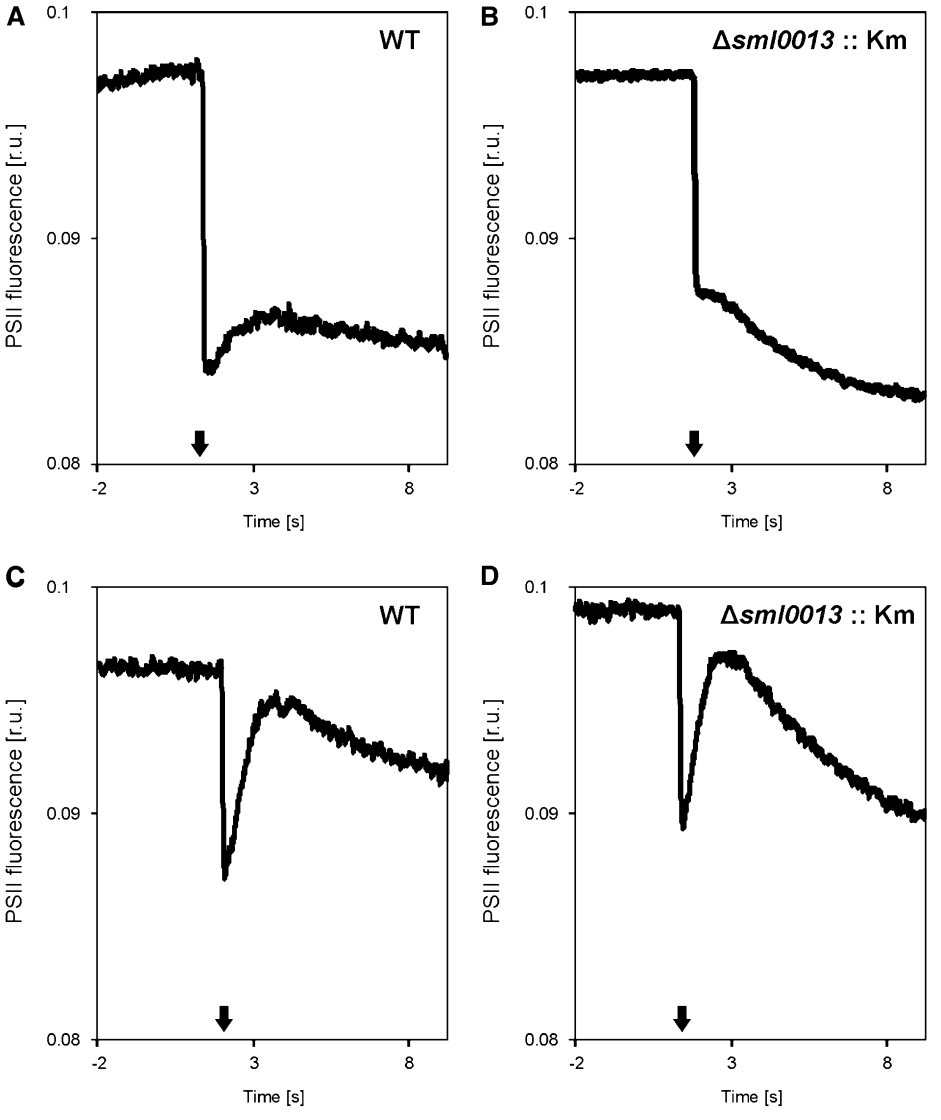

Figure 3. Postillumination (at time point 0 s, actinic light was switched off; black arrows) rise of PSII chlorophyll *a* fluorescence in cells of the *Synechocystis* 6803 wild type (WT) or mutant Δ*sml0013*::Km after growth at HC or LC conditions. A, Wild type at HC. B, Δ*sml0013*::Km at HC. C, Wild type at LC. D, Δ*sml0013*::Km at LC.

PSI Redox Kinetics

Since one main function of NDH1 is participation in the cyclic electron transport around PSI (for review, see Battchikova et al., 2011a), the redox kinetics of PSI were measured using the pulse-amplitude measurement (PAM) technique. In a first attempt, the slow kinetics of PSI oxidation in the presence of a 20-s far-red light treatment were measured with cells of both strains cultivated under HC conditions. The traces of wild-type and mutant cells were almost similar without added inhibitors (Fig. 4), as reported before for mutants of *Synechocystis* 6803 defective in *ndhF* genes (Bernát et al., 2011). The $P700^+$ signal increased after actinic light was switched on and returned to the initial level after it was switched off. To distinguish between electron flow around PSI and electron drain to respiration via Cytox, KCN was added. The addition of KCN changed the redox kinetics of PSI in the wild type, while the traces of the Δ*sml0013*::Km mutant cells remained almost unchanged. The PSI oxidation in wild-type cells almost lost the fast increase after far-red light illumination; instead, it showed a rather slow PSI oxidation increase (Fig. 4). Similar curves were reported by Bernát et al. (2011), where the wild type showed much slower P700 oxidation, whereas it was almost not affected by KCN addition in the Δ*ndhF1/3/4* triple mutant. Obviously, under KCN-free conditions, many electrons are flowing into respiration in wild-type cells; therefore, PSI oxidation was rapid, while inhibited respiration led to a prolonged oxidation time due to increased transfer of electrons toward PSI, which can be a sign for increased cyclic electron transport around PSI or an increased flow of electrons from metabolic activities [e.g. $NAD(P)H+H^+$ produced by catabolic activities] to PSI. This slow increase is almost absent in KCN-treated mutant cells, which indicates that the absence of Sml0013 resulted rather in an impaired electron influx into the PQ pool and not in a changed electron flow to Cytox. The addition of 3-(3,4-dichlorophenyl)-1,1-dimethylurea (DCMU) to KCN-treated cells had only a small impact on the PSI oxidation traces in Δ*sml0013*::Km and wild-type cells. Since it is known that cultivation under different CO_2 amounts changes the composition of the NDH1 (Zhang et al., 2004), we made the same measurements with cell material acclimated long term to LC conditions. These measurements with LC-acclimated cells showed qualitatively the same results (Supplemental Fig. S5) as those with HC cells discussed above.

The quantitative evaluations of the slow PSI redox kinetic measurements supported the visual evaluation (Fig. 5). The decay of the $P700^+$ signal reflecting the electron flow rate to $P700^+$ was slower by about 20% for the mutant Δ*sml0013*::Km compared with the wild type. This difference indicates that fewer electrons reach PSI in mutant cells, supporting the view of a diminished NDH1 function in Δ*sml0013*::Km. The addition of KCN increased the $P700^+$ rereduction rate in wild-type cells as well as mutant cells, because fewer electrons can escape from the cyclic electron flow

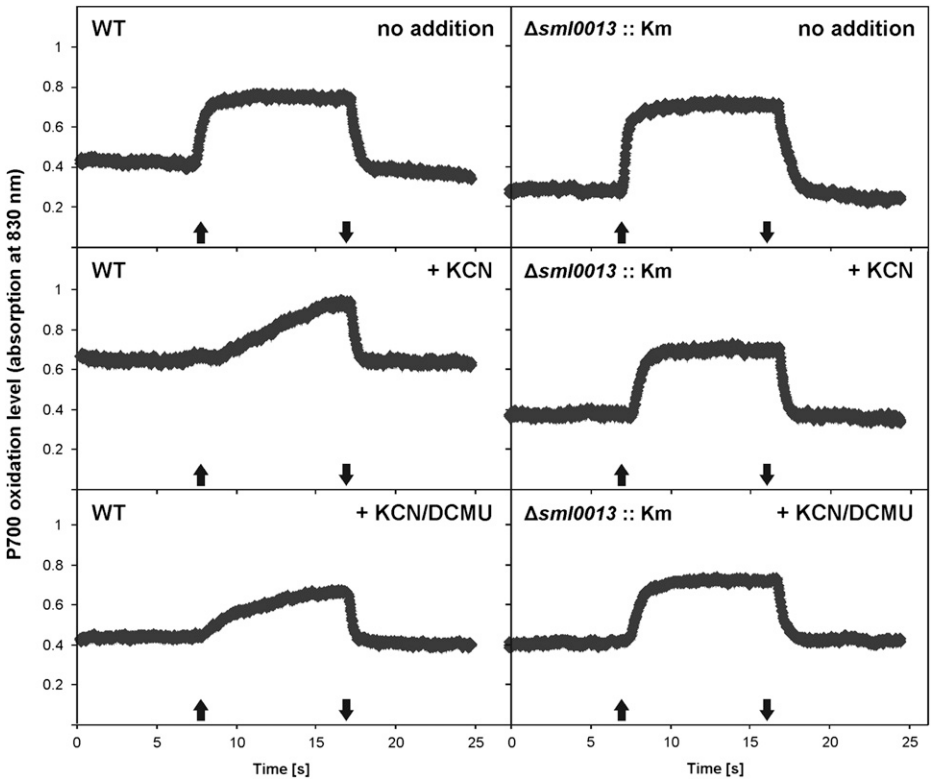

Figure 4. Slow redox kinetics of PSI measured as change in A_{830} after illumination with strong far-red light (710 nm) for 20 s (up and down arrows indicate switching of actinic light on and off). Cells precultured under HC conditions of the wild type (WT) and the mutant Δ*sml0013*::Km were measured without the addition of inhibitors, after the addition of KCN to inhibit electron flow into the respiratory electron chain toward Cytc oxidase, and after combined addition of KCN and DCMU to inhibit both respiratory and photosynthetic linear electron flow from PSII.

around PSI to the Cytox. Interestingly, KCN addition equals the $P700^+$ rereduction rate in both strains. KCN increased the rate almost 2-fold more in cells of Δ*sml0013*::Km compared with the wild type, indicating that more electrons seem to be transferred toward respiration in mutant cells. Alternatively, the rate of PSI rereduction following KCN addition cannot get any faster in either of the two strains, because of a common limitation in electron transfer to PS1. An increased flow to respiration also was shown for the mutant Δ*ndhF1* after KCN addition (Bernát et al., 2011). The final addition of DCMU did not change this rate in the wild type, whereas cells of the mutant decreased the decay somehow, indicating that in these cells some electrons from PSII are reaching PSI even when far-red actinic light is used.

Long-term LC-acclimated cells showed similar trends for the wild type and Δ*sml0013*::Km, albeit the rates were always slower, as in HC cells (Supplemental Fig. S6). Mutant cells always showed slower rereduction rates independent of whether inhibitors were added. KCN addition almost doubled this rate in the two strains; however, the mutant cell rate still was clearly lower than that in wild-type cells. Again, DCMU addition had a much higher effect on the A_{830} decay rate in Δ*sml0013*::Km cells. The $P700^+$ rereduction became even slower than in nontreated cells, while the wild type did not show such a high DCMU effect.

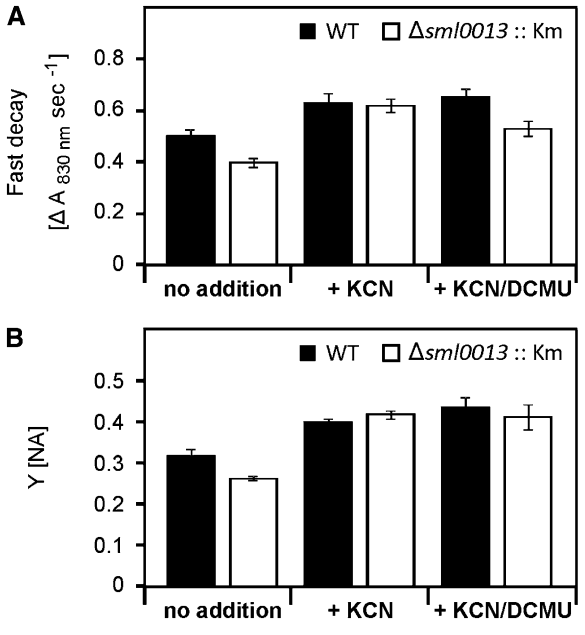

Figure 5. Quantitative evaluation of the measurements of redox kinetics of PSI. Cells precultured under HC conditions of the wild type (WT) and the mutant Δ*sml0013*::Km were measured without the addition of inhibitors, after the addition of KCN to inhibit electron flow into the respiratory electron chain toward Cytc oxidase, and after combined addition of KCN and DCMU to inhibit both respiratory and photosynthetic linear electron flow from PSII. From the slow kinetics, we calculated the rates of the decay phase after switching off far-red light (A). From the fast kinetics, the Y(NA) was calculated (B), reflecting the amount of PSI that can be oxidized under the different conditions. Mean values and SD from one typical experiment are shown ($n = 3$).

Since the addition of DCMU revealed changes in the slow kinetics of P700 oxidation with far-red light, especially with cells of Δ*sml0013*::Km, we assumed that even under this light condition, electrons from PSII are influencing the PSI redox kinetics. Therefore, in another set of PAM experiments to measure fast PSI redox changes, we used an additional white light pulse to obtain a complete oxidation of PSI in cells preilluminated by actinic far-red light, as done before. An immediate rise in A_{830} was observed (Fig. 6; 0.213 ± 0.008 versus 0.135 ± 0.003 for the wild type and Δ*sml0013*::Km when cultivated at LC; 0.221 ± 0.011 versus 0.154 ± 0.005 for the wild type and Δ*sml0013*::Km when grown at HC). This finding indicates that the actinic far-red light was not sufficient to fully oxidize PSI, probably due to a continuous electron inflow to PSI from cyclic electron flow and/or metabolic activities. Moreover, the higher increase in wild-type cells compared with the mutant Δ*sml0013*::Km in the absence of inhibitors implies that a higher amount of electrons from cyclic electron flow and/or metabolism reached PSI in wild-type cells. During the subsequent 200-ms white light pulse, $P700^+$ was expected to become quickly rereduced due to electrons from PSII via linear electron flow. Interestingly, a clear rereduction of $P700^+$ was only observed in mutant cells, while the wild type showed only a very small decrease of A_{830} during the short white-light period. The different behavior during the 200-ms white light pulse indicates a much better coupling of PSII to PSI in mutant compared with wild-type cells. An almost similar picture was observed after the addition of KCN. Again, cells of the mutant Δ*sml0013*::Km showed a clear rereduction of PSI, although with a slightly slower rate, during the 200-ms white light pulse, whereas wild-type cells exhibited only a minor decrease in the PSI oxidation level (Fig. 6). In contrast to Δ*sml0013*::Km, mutants defective in the downstream ORF *sll0514* showed no difference compared with wild-type cells in measurements of fast PSI redox changes (Supplemental Fig. S4).

The Y(NA), which reflects the relative proportion of acceptor-limited PSI centers (i.e. centers in the state $P700\ A^-$), was now similar in HC-grown cells of the mutant compared with the wild type (Fig. 5). This finding can be interpreted as a sign of fewer electrons being drained to Cytox in the wild type compared with the mutant. Finally, cells were treated with KCN and DCMU to block both respiratory and photosynthetic linear electron flow. This treatment abolished the fast rereduction of PSI during the 200-ms pulse in mutant cells almost completely (Fig. 6), verifying that the rereduction of PSI observed in the absence of inhibitors was due to an efficient PSII-to-PSI coupling. However, the DCMU additions had no additional effect on KCN-treated cells of the wild type as well as the mutant regarding the Y(NA) at HC (Fig. 5). The

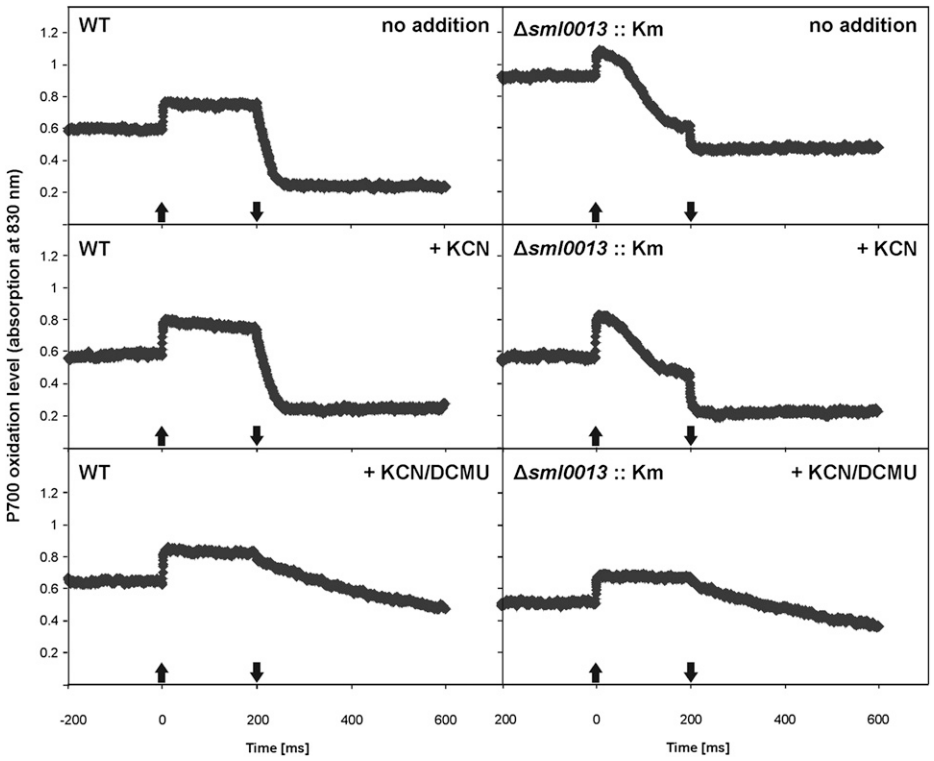

Figure 6. Fast redox kinetics of PSI measured as change in A_{830} after pre-illumination with strong far-red light (710 nm) and a white light pulse of 200 ms (up arrows indicate white light on, and down arrows indicate switching off actinic far-red and white light). Cells precultured under HC conditions of the wild type (WT) and the mutant Δ*sml0013*::Km were measured without the addition of inhibitors, after the addition of KCN to inhibit electron flow into the respiratory electron chain toward Cytc oxidase, and after combined addition of KCN and DCMU to inhibit both respiratory and photosynthetic linear electron flow from PSII.

long-term acclimation to LC resulted in few alterations in the fast PSI reduction measurements. The traces as well as the Y(NA) calculations were very similar to the situation discussed above for HC cells (Supplemental Figs. S6 and S7).

Interestingly, the mutation of *sml0013* improved the coupling of PSII and PSI, because only mutant cells showed a strong $P700^+$ rereduction during the white light pulse independent from the CO_2 content of the preculture. Similarly, the $P700^+$ rereduction rate in measurements of the slow redox kinetics of PSI was also much more strongly influenced by DCMU in mutant than in wild-type cells. One possibility to explain this difference might be different redox levels of the PQ pool. Therefore, the PQ pool was assessed using the method described by Asada et al. (1992). However, these measurements revealed no differences in PQ reduction between wild-type and mutant cells regardless of whether they were grown under HC or LC conditions (data not shown).

CONCLUSION

Short protein-coding genes constitute an abundant, yet largely uncharacterized, fraction in bacterial genomes. The results obtained here suggest that the only 40-amino acid protein Sml0013 is a yet undefined subunit of the cyanobacterial NDH1 complex in *Synechocystis* 6803. It might be involved in the coupling of NDH1 to other electron transport complexes on the thylakoids, thus influencing the relative flux of electrons into the different photosynthetic or respiratory electron transport chains. As proposed before (Nowaczyk et al., 2011), we suggest to name it NdhP. The presence of NdhP homologs in the genome of all 126 cyanobacteria sequenced to date (Shih et al., 2013) indicates an important role of this protein in the natural environment of cyanobacteria. The assumption of an important role of this putative small NDH1 subunit is supported by the notion that NdhP proteins are homologous to NDF6, a subunit of the chloroplastidial NDH complex (Ishikawa et al., 2008). Thus, the chloroplastidial NDH complex, which is evolutionarily and functionally closely related to NDH1 of cyanobacteria (Shikanai, 2007; Ifuku et al., 2011), also kept this small protein subunit despite the long separate evolution.

However, the deletion of NdhP was possible in cells of *Synechocystis* 6803 without affecting cell viability under our standard laboratory conditions. Despite the testing of various growth conditions, only the addition of Glc to cells grown under LC conditions was lethal for the Δ*sml0013*::Km mutant. The presence of Glc has an effect on many different cellular processes, including respiration and photosynthesis (Haimovich-Dayan et al., 2011). It has been shown that the NDH1L complex is not only involved in cyclic electron flow but also required for Glc utilization in *Synechocystis* 6803 (Zhang et al., 2004). Because cultivation under LAHG conditions alleviated the Glc-sensitive phenotype, it can be concluded that neither Glc nor one of its metabolites is directly toxic, but the transfer of electrons from Glc metabolism via an NDH1L complex devoid of NdhP somehow results in overreduction of the electron transfer chain on the thylakoids under light

conditions. Thus, the Glc-sensitive phenotype of the *Synechocystis* 6803 mutant Δ*sml0013*::Km resembles the phenotype reported for many other mutants defective in subunits of the NDH1 complex (for review, see Battchikova et al., 2011a; Haimovich-Dayan et al., 2011).

The rather minor importance of NdhP under our laboratory conditions is reflected by the finding that the overall gene expression pattern was only slightly changed in cells cultivated under HC as well as HC/LC shift conditions. None of the genes for other NDH1 subunits showed any significant difference in the expression level changes in mutant relative to wild-type cells. Interestingly, the gene for the PGR5 homolog in *Synechocystis* 6803 was up-regulated, which correlates with the observed changed activity of cyclic electron flow around PSI in the mutant without NdhP. Additionally, the observed alteration in the phycocyanin/chlorophyll *a* ratio in mutant cells also is in line with the reduced expression of the genes for proteins involved in nitrogen utilization such as *glnA*, *nblA*, and *gifA*.

Despite the rather minor alterations in growth and pigmentation, marked differences were detected in the PSI redox kinetics between wild-type and mutant cells. These experiments showed a decreased activity of cyclic electron flow around PSI, an increased electron transfer out of the photosynthetic into the respiratory electron transfer chain, and an enhanced coupling of PSII to PSI in cells of the mutant Δ*sml0013*::Km. Since defects in the cyclic electron flow around PSI and coupling of the photosynthetic and respiratory electron flow also have been often reported for mutants with missing NDH1L subunits (Battchikova et al., 2011a, 2011b; Bernát et al., 2011; Bolychevtseva et al., 2011), the finding of similar alterations with cells of Δ*sml0013*::Km support our hypothesis that NdhP is functionally associated with the NDH1 in *Synechocystis* 6803. Moreover, the Glc-sensitive phenotype and the absence of marked differences in the PSI redox changes between HC- and LC-acclimated cells make it most likely that NdhP is especially associated with the NDH1L complex (Zhang et al., 2004), which is known to act as part of the joint photosynthetic/respiratory electron flow in *Synechocystis* 6803. Our measurements of PSI redox kinetics suggest that the small NdhP protein possibly somehow improves or even mediates the coupling of PSI and NDH1L, leading to an improved cyclic electron transfer and making it less open for electron entry from PSII or the electron outflow to Cytox, two processes relatively enhanced in the *ndhP* mutant. Whether PSI and NDH1 supercomplexes exist in cyanobacterial cells, as has been shown for plant chloroplasts (Shikanai, 2007), is a matter of discussion that cannot be touched on by our experiments.

MATERIALS AND METHODS

Strains and Cultivation

The Glc-tolerant strain *Synechocystis* sp. PCC 6803 was obtained from Norio Murata (National Institute for Basic Biology) and served as the wild type. Cultures were grown on plates with BG11 medium (Rippka et al., 1979) containing 0.8% agar and buffered with 20 mM TES-KOH to pH 8.0 under constant illumination (30 μmol photons m^{-2} s^{-1}) at 30°C. Cultivation of the mutant Δ*sml0013*::Km was performed in the presence of 50 μg mL^{-1} kanamycin. For the physiological characterization, axenic cultures were grown under light/dark regimes: (1) continuous light at 50 μmol photons m^{-2} s^{-1}; (2) diurnal light/dark cycles (12 h of light/12 h of dark); and (3) complete darkness with a 20-min light pulse at 50 μmol photons m^{-2} s^{-1} every 24 h (LAHG; Anderson and McIntosh, 1991). Growth experiments on plates or in shaken flasks were performed under controlled conditions in the climate cabinet BrightBoy GroBank Mobylux BB-XXL^{3+} (CLF Plant Climatics). To grow cells under photoheterotrophic or LAHG conditions, the BG11 medium was supplemented with 10 mM Glc. To test the axenic character of the cyanobacterial culture, 20 μL of the culture was dropped onto a plate with Luria-Bertani medium and cultivated at 30°C for 48 h.

To obtain higher amounts of biomass, cells were grown photoautotrophically in batch cultures using glass vessels of 3 cm diameter with 5-mm glass tubes for aeration (blubbing flow rate was 5 mL min^{-1}) under continuous illumination of 130 μmol photons m^{-2} s^{-1} (Osram L58 W 32/3) at 29°C. For CO_2 shift experiments, cells were precultivated with air enriched with 5% CO_2 (defined as HC) in BG11 medium of pH 8.0. Then, cells were harvested by centrifugation (5 min at 3,000*g*, 20°C). The pellet was washed and resuspended in fresh BG11 medium of pH 7.0 at an optical density at 750 nm of 0.8. After 1 h of cultivation under HC conditions, CO_2 limitation was set by shifting the exponentially growing cultures to bubbling with ambient air containing 0.038% CO_2 (defined as LC). For long-term acclimation to HC or LC, cells were cultivated under the defined conditions for 72 h. The suspensions were daily diluted to an optical density at 750 nm of 0.8 by the corresponding medium.

Generation of Mutants

Total DNA from *Synechocystis* 6803 was isolated according to Hagemann et al. (1997). All other DNA techniques, such as ligation, plasmid isolation, restriction analysis, and transformation of *Escherichia coli*, were standard methods (Sambrook et al., 1989). To delete the gene *sml0013*, the encoding sequence together with approximately 750 bp of upstream or downstream sequences were amplified using specific oligonucleotide primers (Supplemental Table S1) via PCR. PCR was carried out using the *Taq*-PCR Master Mix (Qiagen) and additionally Elongase Enzyme Mix (Invitrogen). The fragments were separately cloned into the pGEMT (Promega) vector, resulting in pGEMT-*sml0013*-up as well as pGEMT-*sml0013*-down. To combine upstream and downstream sequences, first the pGEMT-*sml0013*-down vector was cut with *Nhe*I and *Nde*I. Then, the pGEMT-*sml0013*-up vector was cut with *Xba*I and *Nde*I to obtain the *sml0013* upstream genome area. This fragment was inserted into the pGEMT-*sml0013*-down vector. The coding sequence of *sml0013* was replaced by the *aphII* gene cartridge (for aminoglycoside phosphotransferase II, conferring kanamycin resistance), which was excised from pUC4K (Pharmacia) with *Stu*I and *Bam*HI. This kanamycin resistance cartridge was inserted into the *Cla*I cutpGEMT-*sml0013*-up-down vector (carrying the upstream and downstream *sml0013*-localized genome area). To obtain compatible ends for ligation, 5′ overhangs were filled in using the Klenow enzyme (Fermentas). The final insert was verified by DNA sequencing (Seqlab). The transformation of wild-type *Synechocystis* 6803 with the generated mutation was done as described by Hagemann and Zuther (1992). The genotype and complete segregation of the *Synechocystis* 6803 mutant Δ*sml0013*::Km were checked by PCR using the primers *sml0013*_fw and *sml0013*_rev (Supplemental Table S1). Only DNA fragments with sizes corresponding to the mutated genes were detected with DNA from mutant clones, whereas fragments of wild-type gene sizes were completely absent (Supplemental Fig. S3).

To rule out polar effects, mutants defective in *sll0514*, which represents the ORF downstream of *sml0013*, were generated. The wild-type fragment of *sll0514* was generated by PCR and cloned into pGEMT (Promega). The mutant Δ*sll0514*::SmI was generated by insertion of the spectinomycin resistance cartridge obtained from pUC4S into the uncial *Bam*HI site of *sll0514*. The mutant Δ*sll0514*::SmD was generated by deletion of the 671-bp *Hpa*I/*Sma*I fragment from *sll0514* and its subsequent replacement by the spectinomycin resistance cartridge. The genotype and complete segregation of the *Synechocystis* 6803 mutants Δ*sll0514*::SmI and Δ*sll0514*::SmD were checked by PCR using the primers *sll0514*_fw and *sll0514*_rev (Supplemental Table S1). Only DNA fragments with sizes corresponding to the mutated genes were detected

with DNA from mutant clones, whereas fragments of wild-type gene sizes were completely absent (Supplemental Fig. S4).

Sequence comparisons were done using the BLAST algorithm (Altschul et al., 1997) at the National Center for Biotechnology Information (http://www.ncbi.nlm.nih.gov). Cyanobacterial genome sequences were analyzed and extracted from CyanoBase (http://genome.microbedb.jp/cyanobase).

DNA Microarray to Characterize Gene Expression Changes

Cells from 5 mL of culture were harvested by centrifugation at 4,000 rpm for 5 min at 4°C and were immediately frozen at −80°C. Total RNA was extracted after pretreatment with hot phenol and chloroform by the High PureRNA isolation kit (Roche Diagnostics). Transcriptome analysis was done using custom-made 4x44K Agilent RNA microarrays. In addition to probes for protein-coding genes, the microarray contains probes for noncoding RNAs and untranslated regions of the *Synechocystis* 6803 chromosome (GenBank accession no. NC_000911.1) and plasmid pSYSA (NC_005230) as identified by Mitschke et al. (2011). Each probe has an internal technical duplicate. The detailed description and probe sequences are deposited in the GEO database under accession number GPL15867.

Hybridization of the microarrays was done according to Georg et al. (2009). Two micrograms of RNA was directly labeled with Cy3 using the Kreatech "ULS labeling kit for Agilent gene expression arrays." Then, 1.65 μg of the labeled RNA was hybridized to each microarray following the Agilent protocol for single-color microarrays. The microarrays were digitalized with an Agilent G2565CA Microarray Scanner using the Agilent Feature Extraction Software 10.7.3.1 and protocol GE1_107_Sep09. The raw data were quantile normalized with the R package *limma*. The probe sets for the different RNA features were averaged before the summarization of the biological replicates and contrast extraction by *limma*. Each experiment was performed with RNA from two biological replicates. The microarray data are accessible in the GEO database under accession number GSE48415.

PAM to Characterize NDH1 and PSI Redox Kinetics

The postillumination rise in chlorophyll *a* fluorescence after actinic light had been switched off was measured according to Ma and Mi (2005) by means of a Dual PAM (Walz). After dark acclimation for 30 min, samples were exposed to actinic red light (approximately 630 nm, 95 μmol photons m^{-2} s^{-1}) for 30 s, and the kinetic of PSII chlorophyll fluorescence after switching off actinic illumination was recorded as a measure of NDH activity (Battchikova et al., 2011b). Measurements were done at low measuring light (7 μmol photons m^{-2} s^{-1}) and low measuring frequency (2,000 Hz) in order to achieve undisturbed postillumination signals.

For measurements of the redox kinetics of PSI, we used the Dual PAM (Walz). Cell suspensions precultivated to either HC or LC conditions were directly taken from the culture vessels at a density of approximately 5 μg chlorophyll *a* mL^{-1}. P700 redox kinetics (called "slow redox kinetics" hereafter) were recorded in a stirred 4-mL cuvette as described by Ma et al. (2008) after 20 min of preincubation in darkness. A far-red illumination (more than 705 nm, 75 W m^{-2}) was provided for 20 s, oxidizing P700 to a steady state. Because far-red light excites almost exclusively PSI, electron donation by PSII can be neglected. Therefore, the rate of $P700^+$ formation after the onset of far-red illumination ("initial fast increase") provides information about the electron transport through the PQ pool and $Cytb_6f$; the addition of KCN (final concentration, 1 mM) allowed for discrimination between PSI- and Cytox-directed electron transport. After the initial fast increase, caused by rapid emptying of both PQ pool- as well as $Cytb_6f$-stored electrons, a second, slow increase in $P700^+$ could be observed ("slow increase") until reaching a steady-state level of $P700^+$ (Pm′; Klughammer and Schreiber, 2008). After switching off the far-red actinic light, the $P700^+$ rereduction kinetics were followed and quantitatively evaluated.

Since the far-red light-induced Pm′ does not reflect full P700 oxidation level because of remaining PSII activity, cyclic electron transport, and electron flow from metabolites to PQ via respiratory enzymes (Klughammer and Schreiber, 1994, 2008; Bernát et al., 2011), processes contributing to the slow increase, a strong, white light illumination pulse (18,000 μmol photons m^{-2} s^{-1} for 200 ms) was applied to allow the determination of maximum $P700^+$ level (Pm), which can be derived by the extrapolation routine of the Dual-PAM software as described by Klughammer and Schreiber (2008). After onset of the saturation pulse, the $P700^+$ level rises to a maximum followed by a biphasic decrease. Whereas the second phase, starting about 30 ms after the onset of illumination, is believed to reflect the rereduction of $P700^+$ by electrons generated by PSII (Klughammer and Schreiber, 1994), the first phase indicates the existence of a rapid type of cyclic PSI flow (Klughammer and Schreiber, 1994, 2008). The addition of DCMU (final concentration, 0.1 mM) and KCN (final concentration, 1 mM) blocked any remaining contribution from PSII as well as the loss of electrons to the respiratory terminal electron acceptor. Therefore, the $P700^+$ reduction kinetics in the presence of both inhibitors reflects the donation of electrons stored in cyclic pathways and electrons generated de novo by respiratory enzymes. From these measurements, we calculated the Y(NA) as $(Pm - Pm')/(Pm - P_0)$ (P0–P700 oxidation level in darkness; Klughammer and Schreiber, 2008).

Supplemental Data

The following materials are available in the online version of this article.

Supplemental Figure S1. Multiple alignment of cyanobacterial Sml0013-like proteins.

Supplemental Figure S2. Multiple alignment of NDF6-like proteins of plants, cyanobacteria, and a cyanophage.

Supplemental Figure S3. Deletion of the gene *sml0013* in *Synechocystis* 6803 to generate the mutant Δ*sml0013*::Km.

Supplemental Figure S4. Deletion of the gene *sll0514* in *Synechocystis* 6803 to generate the mutant Δ*sml0514*::Sm.

Supplemental Figure S5. Traces of the slow redox kinetics of PSI of long-term LC-acclimated cells.

Supplemental Figure S6. Quantitative evaluation of the measurements of the redox kinetics of PSI with long-term LC-acclimated cells.

Supplemental Figure S7. Traces of the fast redox kinetics of PSI of long-term LC-acclimated cells.

Supplemental Table S1. Primers used to generate the *Synechocystis* 6803 mutants.

Supplemental Table S2. List of noncoding or antisense transcripts showing significant transcriptional changes in cells of the *Synechocystis* 6803 mutant Δ*sml0013*::Km.

Supplemental File S1. Graphical representation of the entire genome of *Synechocystis* 6803 and the fold change values for each microarray probe.

ACKNOWLEDGMENTS

The excellent technical assistance of Klaudia Michl is highly appreciated. We also thank Teruo Ogawa, who introduced M.H. to the various functions of cyanobacterial NDH1.

Received July 1, 2013; accepted October 1, 2013; published October 2, 2013.

LITERATURE CITED

Aguirre von Wobeser E, Ibelings BW, Bok J, Krasikov V, Huisman J, Matthijs HCP (2011) Concerted changes in gene expression and cell physiology of the cyanobacterium *Synechocystis* sp. strain PCC 6803 during transitions between nitrogen and light-limited growth. Plant Physiol **155:** 1445–1457

Altschul SF, Madden TL, Schäffer AA, Zhang J, Zhang Z, Miller W, Lipman DJ (1997) Gapped BLAST and PSI-BLAST: a new generation of protein database search programs. Nucleic Acids Res **25:** 3389–3402

Anderson SL, McIntosh L (1991) Light-activated heterotrophic growth of the cyanobacterium *Synechocystis* sp. strain PCC 6803: a blue-light-requiring process. J Bacteriol **173:** 2761–2767

Asada K, Heber U, Schreiber U (1992) Pool size of electrons that can be donated to $P700^+$ as determined in intact leaves: donation to $P700^+$ from stromal components via the intersystem chain. Plant Cell Physiol **33:** 927–932

Baier K, Nicklisch S, Grundner C, Reinecke J, Lockau W (2001) Expression of two *nblA*-homologous genes is required for phycobilisome degradation in nitrogen-starved *Synechocystis* sp. PCC6803. FEMS Microbiol Lett **195:** 35–39

Battchikova N, Eisenhut M, Aro EM (2011a) Cyanobacterial NDH-1 complexes: novel insights and remaining puzzles. Biochim Biophys Acta **1807:** 935–944

Battchikova N, Wei L, Du L, Bersanini L, Aro EM, Ma W (2011b) Identification of novel Ssl0352 protein (NdhS), essential for efficient operation of cyclic electron transport around photosystem I, in NADPH:plastoquinone oxidoreductase (NDH-1) complexes of *Synechocystis* sp. PCC 6803. J Biol Chem **286:** 36992–37001

Bernát G, Appel J, Ogawa T, Rögner M (2011) Distinct roles of multiple NDH-1 complexes in the cyanobacterial electron transport network as revealed by kinetic analysis of $P700^+$ reduction in various Ndh-deficient mutants of *Synechocystis* sp. strain PCC6803. J Bacteriol **193:** 292–295

Bolychevtseva YV, Elanskaya IV, Karapetyan NV (2011) Regulation of cyclic electron transport through photosystem I in cyanobacterium *Synechocystis* sp. PCC 6803 mutants deficient in respiratory dehydrogenases. Biochemistry (Mosc) **76:** 427–437

Bryant DA (1994) The Molecular Biology of Cyanobacteria. Kluwer Academic Publishers, Dordrecht, The Netherlands

Cobley J (2010) A gene required for photoregulation of phycobilisome abundances and for heterotrophic growth in *Fremyella diplosiphon* is present in all cyanobacterial genomes and in the genome of some cyanophages. *In* C Kerfeld, D Schluchter, eds, Abstract at the 10th Cyanobacterial Molecular Biology Workshop, Lake Arrowhead, California, USA, p 38

Collier JL, Grossman AR (1994) A small polypeptide triggers complete degradation of light-harvesting phycobiliproteins in nutrient-deprived cyanobacteria. EMBO J **13:** 1039–1047

Eisenhut M, Aguirre von Wobeser E, Jonas L, Schubert H, Ibelings BW, Bauwe H, Matthijs HC, Hagemann M (2007) Long-term response toward inorganic carbon limitation in wild type and glycolate turnover mutants of the cyanobacterium *Synechocystis* sp. strain PCC 6803. Plant Physiol **144:** 1946–1959

Eisenhut M, Georg J, Klähn S, Sakurai I, Mustila H, Zhang P, Hess WR, Aro EM (2012) The antisense RNA As1_flv4 in the Cyanobacterium *Synechocystis* sp. PCC 6803 prevents premature expression of the *flv4-2* operon upon shift in inorganic carbon supply. J Biol Chem **287:** 33153–33162

Engelken J, Funk C, Adamska I (2012) The extended light-harvesting complex (LHC) protein superfamily: classification and evolutionary dynamics. *In* RL Burnap, WFJ Vermaas, eds, Functional Genomics and Evolution of Photosynthetic Systems: Advances in Photosynthesis and Respiration, Vol 33. Springer, Dordrecht, The Netherlands, pp 265–284

Funk C, Vermaas WFJ (1999) A cyanobacterial gene family coding for single-helix proteins resembling part of the light-harvesting proteins from higher plants. Biochemistry **38:** 9397–9404

García-Domínguez M, Reyes JC, Florencio FJ (2000) NtcA represses transcription of *gifA* and *gifB*, genes that encode inhibitors of glutamine synthetase type I from *Synechocystis* sp. PCC 6803. Mol Microbiol **35:** 1192–1201

Georg J, Voss B, Scholz I, Mitschke J, Wilde A, Hess WR (2009) Evidence for a major role of antisense RNAs in cyanobacterial gene regulation. Mol Syst Biol **5:** 305

Gupta RS, Mathews DW (2010) Signature proteins for the major clades of cyanobacteria. BMC Evol Biol **10:** 24

Hagemann M, Jeanjean R, Fulda S, Havaux M, Erdmann N (1999) Flavodoxin accumulation contributes to enhanced cyclic electron flow around photosystem I in salt-stressed cells of *Synechocystis* sp. PCC 6803. Physiol Plant **105:** 670–678

Hagemann M, Schoor A, Jeanjean R, Zuther E, Joset F (1997) The stpA gene from *Synechocystis* sp. strain PCC 6803 encodes the glucosylglycerolphosphate phosphatase involved in cyanobacterial osmotic response to salt shock. J Bacteriol **179:** 1727–1733

Hagemann M, Zuther E (1992) Selection and characterization of mutants of the cyanobacterium *Synechocystis* sp. PCC 6803 unable to tolerate high salt concentrations. Arch Microbiol **158:** 429–434

Haimovich-Dayan M, Kahlon S, Hihara Y, Hagemann M, Ogawa T, Ohad I, Lieman-Hurwitz J, Kaplan A (2011) Cross-talk between photomixotrophic growth and CO_2 -concentrating mechanism in *Synechocystis* sp. strain PCC 6803. Environ Microbiol **13:** 1767–1777

Hu P, Lv J, Fu P, Hualing M (2013) Enzymatic characterization of an active NDH complex from *Thermosynechococcus elongatus*. FEBS Lett **587:** 2340–2345

Ifuku K, Endo T, Shikanai T, Aro EM (2011) Structure of the chloroplast NADH dehydrogenase-like complex: nomenclature for nuclear-encoded subunits. Plant Cell Physiol **52:** 1560–1568

Ishikawa N, Takabayashi A, Ishida S, Hano Y, Endo T, Sato F (2008) NDF6: a thylakoid protein specific to terrestrial plants is essential for activity of chloroplastic NAD(P)H dehydrogenase in Arabidopsis. Plant Cell Physiol **49:** 1066–1073

Klughammer C, Schreiber U (1994) An improved method, using saturating light pulses, for the determination of photosystem I quantum yield via $P700^+$-absorbance changes at 830 nm. Planta **192:** 261–268

Klughammer C, Schreiber U (2008) Saturation pulse method for assessment of energy conversion in PSI. PAM Application Notes **1:** 11–14

Larsson J, Nylander JA, Bergman B (2011) Genome fluctuations in cyanobacteria reflect evolutionary, developmental and adaptive traits. BMC Evol Biol **11:** 187

Los DA, Suzuki I, Zinchenko VV, Murata N (2008) Stress responses in *Synechocystis*: regulated genes and regulatory systems. *In* A Herrero, E Flores, eds, The Cyanobacteria: Molecular Biology, Genomics and Evolution. Caister Academic Press, Norfolk, UK, pp 117–158

Ma WM, Mi HL (2005) Expression and activity of type 1 NAD(P)H dehydrogenase at different growth phases of the cyanobacterium *Synechocystis* PCC 6803. Physiol Plant **125:** 135–140

Ma WM, Wei LZ, Wang QX (2008) The response of electron transport mediated by active NADPH dehydrogenase complexes to heat stress in the cyanobacterium *Synechocystis* 6803. Sci China C Life Sci **51:** 1082–1087

Mitschke J, Georg J, Scholz I, Sharma CM, Dienst D, Bantscheff J, Voss B, Steglich C, Wilde A, Vogel J, et al (2011) An experimentally anchored map of transcriptional start sites in the model cyanobacterium *Synechocystis* sp. PCC6803. Proc Natl Acad Sci USA **108:** 2124–2129

Munekage Y, Hojo M, Meurer J, Endo T, Tasaka M, Shikanai T (2002) PGR5 is involved in cyclic electron flow around photosystem I and is essential for photoprotection in *Arabidopsis*. Cell **110:** 361–371

Nowaczyk MM, Wulfhorst H, Ryan CM, Souda P, Zhang H, Cramer WA, Whitelegge JP (2011) NdhP and NdhQ: two novel small subunits of the cyanobacterial NDH-1 complex. Biochemistry **50:** 1121–1124

Ogawa T (1991) A gene homologous to the subunit-2 gene of NADH dehydrogenase is essential to inorganic carbon transport of *Synechocystis* PCC6803. Proc Natl Acad Sci USA **88:** 4275–4279

Peschek GA, Obinger C, Fromwald S, Bergman B (1994) Correlation between immuno-gold labels and activities of the cytochrome-c oxidase (aa3-type) in membranes of salt stressed cyanobacteria. FEMS Microbiol Lett **124:** 431–437

Pils D, Schmetterer G (2001) Characterization of three bioenergetically active respiratory terminal oxidases in the cyanobacterium *Synechocystis* sp. strain PCC 6803. FEMS Microbiol Lett **203:** 217–222

Rippka R, Deruelles J, Waterbury JB, Herdman M, Stanier RY (1979) Generic assignments, strain histories and properties of pure cultures of cyanobacteria. Microbiology **111:** 1–61

Sambrook J, Fritsch EF, Maniatis T (1989) Molecular Cloning. Cold Spring Harbor Laboratory Press, Cold Spring Harbor, NY

Scanlan DJ, Ostrowski M, Mazard S, Dufresne A, Garczarek L, Hess WR, Post AF, Hagemann M, Paulsen I, Partensky F (2009) Ecological genomics of marine picocyanobacteria. Microbiol Mol Biol Rev **73:** 249–299

Shibata M, Ohkawa H, Kaneko T, Fukuzawa H, Tabata S, Kaplan A, Ogawa T (2001) Distinct constitutive and low-CO_2-induced CO_2 uptake systems in cyanobacteria: genes involved and their phylogenetic relationship with homologous genes in other organisms. Proc Natl Acad Sci USA **98:** 11789–11794

Shih PM, Wu D, Latifi A, Axen SD, Fewer DP, Talla E, Calteau A, Cai F, Tandeau de Marsac N, Rippka R, et al (2013) Improving the coverage of the cyanobacterial phylum using diversity-driven genome sequencing. Proc Natl Acad Sci USA **110:** 1053–1058

Shikanai T (2007) Cyclic electron transport around photosystem I: genetic approaches. Annu Rev Plant Biol **58:** 199–217

Wang HL, Postier BL, Burnap RL (2004) Alterations in global patterns of gene expression in *Synechocystis* sp. PCC 6803 in response to inorganic carbon limitation and the inactivation of *ndhR*, a LysR family regulator. J Biol Chem **279:** 5739–5751

Yamamoto H, Peng L, Fukao Y, Shikanai T (2011) An Src homology 3 domain-like fold protein forms a ferredoxin binding site for the chloroplast NADH dehydrogenase-like complex in *Arabidopsis*. Plant Cell **23:** 1480–1493

Yeremenko N, Jeanjean R, Prommeenate P, Krasikov V, Nixon PJ, Vermaas WFJ, Havaux M, Matthijs HCP (2005) Open reading frame *ssr2016* is required for antimycin A-sensitive photosystem I-driven cyclic electron flow in the cyanobacterium *Synechocystis* sp. PCC 6803. Plant Cell Physiol **46:** 1433–1436

Zhang P, Battchikova N, Jansen T, Appel J, Ogawa T, Aro EM (2004) Expression and functional roles of the two distinct NDH-1 complexes and the carbon acquisition complex NdhD3/NdhF3/CupA/Sll1735 in *Synechocystis* sp PCC 6803. Plant Cell **16:** 3326–3340